



## CUTTING TOOL LIFE AND ITS EFFECT ON SURFACE ROUGHNESS WHEN TURNING WITH WC-6% CO

Mourad Bendifallah<sup>1</sup>, Mourad Brioua<sup>1</sup>, Abderrahim Belloufi<sup>2</sup>

<sup>1</sup> University of Mostefa Ben Boulaïd Batna 2, Faculty of Technology, Laboratory of Innovation in Construction, Eco-design and Seismic Engineering, Department of Mechanics, Batna 05078, Algeria

<sup>2</sup> University of Kasdi Merbah Ouargla, Faculty of Applied Sciences, Department of Mechanical Engineering, Ouargla 30000, Algeria

Corresponding author: Abderrahim Belloufi, abelloufi@yahoo.fr

**Abstract:** During turning operations, tool-part-chip contact causes wear to the cutting tool. The objective of this work is to study the wear of the clearance faces of tungsten carbide cutting tools during turning operations. Experimental tests on tool life for dry turning operations were carried out at four different cutting speeds, where the feed rate and the depth of cut are kept at constant values: 0.08 mm/rev for feed rate and 0.5 mm for depth of cut. An analysis of the influence of cutting parameters on the tools wear and consequently tool life (T) was presented, then the roughness of the machined surface Ra and the morphology of the chips produced were studied. This study makes it possible to identify that the wear mechanisms and the tool life are strongly linked to the roughness of the machined surfaces and to the morphology of the chips produced during the turning operations.

**Key words:** Turning, WC-Co, Tool wear, roughness, Chips, High speed steel, Tool life

### NOMENCLATURE

HS18-0-1	high-speed steel workpieces
WC-Co	Cutting tool material
Vc	Cutting speed (m/min)
f	Feed rate (mm/rev)
a <sub>p</sub>	Depth of cut (mm)
T	Tool life
VB	Flank wear
Ra	Arithmetic mean roughness (μm)
Rz	Mean depth roughness (μm)

### 1. INTRODUCTION

Over the last few decades, there has been a great deal of research into conventional machining to improve machinability. Many researchers have used different materials for cutting tools in turning cutting research [1, 2].

The monitoring of the condition of cutting tool plays an important role during the cutting process, therefore the achievement of constant quality such as dimensional accuracy, surface roughness and control of the total

manufacturing cost depends mainly on the condition of the cutting tool and therefore the cutting process requires a good evaluation of the cutting tool, [3].

Tungsten carbide is a composite material produced by powder metallurgy using liquid phase sintering. It offers the rigidity and strength of common materials for applications requiring wear resistance, such as machine tools. WC-Co typically contains about 4-12 wt.% Co-Binder and WC grain size is typically between 0.5 and 10 μm [4].

Several studies have been carried out on tool life and wear development of tools when turning tungsten carbide [5-7]. Usually, the cutting tool wears in each of the contact areas and appears in several forms, such as face wear, crater wear, chipping, etc., which can be caused by the cutting tool [8]. These shapes depend mainly on the characteristics of the cutting tool, the material of the workpiece, the cutting conditions, and the types of cutting [9].

According to ISO 3685 (1993), face wear is considered to be the most important during normal machining conditions, the measurement of the face wear width (FWW) is the most commonly used parameter for evaluating the service life of a cutting tool [10]. In case of uneven wear, the maximum width of the wear zone (VB<sub>max</sub>) should be less than 0.6 mm [11]. The development of this form of wear on the cutting tool is not a random phenomenon. A typical evolution of the frontal wear area (VB) with the cutting time for different cutting speeds. Wear can be divided into three zones during its service life [12].

- Initial wear zone which is caused by the initial breakage of the sharp corners of the cutting edge. The edge is then stabilized and wear occurs by gradual removal of material from the tool.
- Regular wear zone, which corresponds to wear at a uniform rate, represents the useful life of the cutting edge.
- Accelerated wear zone, where wear occurs progressively.

In general, the assessment of cutting tool wear can be done in two ways: direct and indirect. The direct methods consist of measuring the state of wear of the tool using conventional vision or optical systems such as cameras, equipped optical microscopes and/or white light interferometers. These methods have the advantage of measuring the exact geometrical changes due to cutting tool wear [13].

Undercutting wear, also known as face wear, results wear between the tool face and the workpiece. This type of wear is mainly due to purely mechanical mechanisms that are favored when cutting materials. Consequently, flank wears acts directly on the surface integrity of the machined workpiece and its dimensional accuracy [14]. On the face of the wear zone, the wear is characterised by a uniform height of the wear zone of the cutting tool. This medium length is frequently designated as VB [15].

One of the most important fundamental elements in obtaining a high quality product is the cutting tool: its quality and life cycle management directly refer to the efficiency of the whole manufacturing process [16]. Wear is one of the most important problems in the design of cutting operations, a tool is considered worn when the cost of its replacement is less than its cost of use, [17].

Tool failure is said to occur when the tool no longer performs the desired function, while total failure (ultimate failure) is considered to be the total elimination of the cutting edge, a condition that occurs when catastrophic failure occurs [18]. Therefore, cutting tools change ahead of total wear to avoid the elaborate costs and failures of this process. [19]. Selected tool life rejection factors presented in ISO 3685 are listed below [20, 21]:

1. Average Flank wear= 0.4 mm
2. Maximum Flank wear = 0.6 mm
3. Notch = 1.0 mm
4. Nose wear = 0.5 mm
5. Surface roughness (Ra) = 6.0  $\mu\text{m}$ . [22]

However, in case the wear distribution on the face is not homogeneous, a parameter denoted VB is introduced to measure the maximum height of the wear strip [23-25]. Sometimes a notch of VB height is formed on the flank at the cutting edge, which weakens the cutting edge considerably [26-29].

It is important to note that the VB parameter is preferred for tool life characterization due to progressive and easily measurable wear on the face [30-33].

This paper presents a study of cutting tool life; flank wear; surface roughness, and chip morphology when dry turning HS18-0-1 steel with a tungsten carbide (WC-6%Co) tool.

For a better comprehension of the cutting process, the roughness of the machined parts, the wear mechanisms of the tools and the morphology of the generated chips were analyzed. Experiments were executed to study the

consequent effect of the cutting parameters on the tool and the workpiece in terms of flank wear and surface roughness (cutting speed, cutting time).

## 2. EXPERIMENTAL METHOD

### 2.1 Materials and equipment

All experiments carried out under industrial conditions using a AL-PIN lathe machine, model 250, with a spindle power of 6.6 kW as shown in Figure 1.



Fig. 1. AL-PIN lathe machine

The experiments were carried out by machining prismatic parts of High Speed Steel HS18-0-1 (AISI T1).

AISI T1 is mainly used for the manufacture of cutting tools (drills, saws, milling cutters, punch ...). In these steels the addition of tungsten significantly increases its hardness and resistance to high temperature. AISI T1 has excellent resistance to thermal shock and thermal fatigue. Their resistance to high temperature, their toughness and their ability to polish allow them to respond to the most severe demands. This steel has exceptional wear resistance and compression qualities. The hardness of these steels is about 250 HB.

Despite their poor machinability, the machining of this steel shows substantial advantages in terms of surface integrity, more flexibility and lower cost price.

The chemical composition of AISI T1 High Speed Steel is described in Table 1.

Table 1. Chemical composition of machined steel

Element	C	Cr	W	Mo	V
Content (%)	0.8%	4%	18%	0%	1.1%

There are a variety of materials that can be used as cutting tools for turning such as metal carbides. These different carbides are mainly tungsten (WC), titanium (TiC), tantalum (TaC) and niobium (NbC) carbides. The wafers used in this experiment are tungsten carbides of designation WC-Co; of designation WNMM080404-PF.

Chip morphology is examined using an optical microscope of the CMM type, equipped with a CCD camera.

For the measurement of the volumetric wear, the inserts are carefully cleaned and weighed after each pass with an OHAUS balance with a precision of 0.0001mg is used. The inserts were weighed before

and after the machining of each experiment to determine the weight loss.

For the direct measurement of wear (VB) an Optiv Performance 443 Dual Z combines optical and tactile measurement in one system is used (Figure 2). The system supports multi-sensor measurements using the Vision-Sensor, the touch-trigger and scanning probe, the TTL laser (Through-The-Lens) as well as the innovative Chromatic White Light Sensor (CWS). Measurement software is PC-DMIS Vision. Its characteristic is given in Table 2.

Table 2. Characteristic of the MMT OPTV used

Working conditions	Description
Wavelength of red laser	650 nm to 680 nm
Taille du spot	50 $\mu$ m to 100 $\mu$ m
Resolution of the scale	10 nm
Loading capacity	30 kg
Vision-Sensor	3 rings of (27°, 35°, 45°)
Camera zoom CNC	(H 752 x V 582 pixels) x 10



Fig. 2. MMT OPTV performance 443 dual z

For surface measurement a roughness meter a roughnessmeter (2D), equipped with a roughness profile printer, shown in Figure 3 is used. It consists of a stylus that moves mechanically over a surface to record the roughness of the surface over a determined sample length.

The latter consists of a diamond tip (probe), with a tip radius of 5 $\mu$ m moving linearly over the measured surface.

The probing length is 4 mm with a base length of 0.8 mm. The measuring interval of the roughness criteria is (0.05 to 40 $\mu$ m). In order to avoid rework errors and for greater accuracy, the roughness measurement was carried out directly on the machine and without dismantling the workpiece.



Fig. 3. Roughness measurement

## 2.2 Experimental setup

Forty (40) experiments were carried out, in dry conditions, using one input (control) parameter: cutting speed. This parameter varies to four discrete level values: 380 m/min, 620 m/min, 760 m/min and 1100 m/min.

There are many cutting parameters that affect cutting tool life. Cutting speed is the most active influence parameter on cutting tool life. Advantageously, this parameter is also the easiest to adjust, and can directly modify their value in lath machine with no additional cost. Thus, other important parameters were not considered (feed rate and depth of cut) whose values were kept constant throughout experiments. The constant conditions and corresponding values were  $f = 0.08$  mm/rev and  $a_p = 0.5$  mm.

Measurements are taken after each pass, with 10 passes approved for each cutting speed.

The experimental setup used in this study is presented in Figure 4. This configuration illustrates, in a simplified manner, the steps to be followed to carry out the experimental tests and the various materials used in these tests.

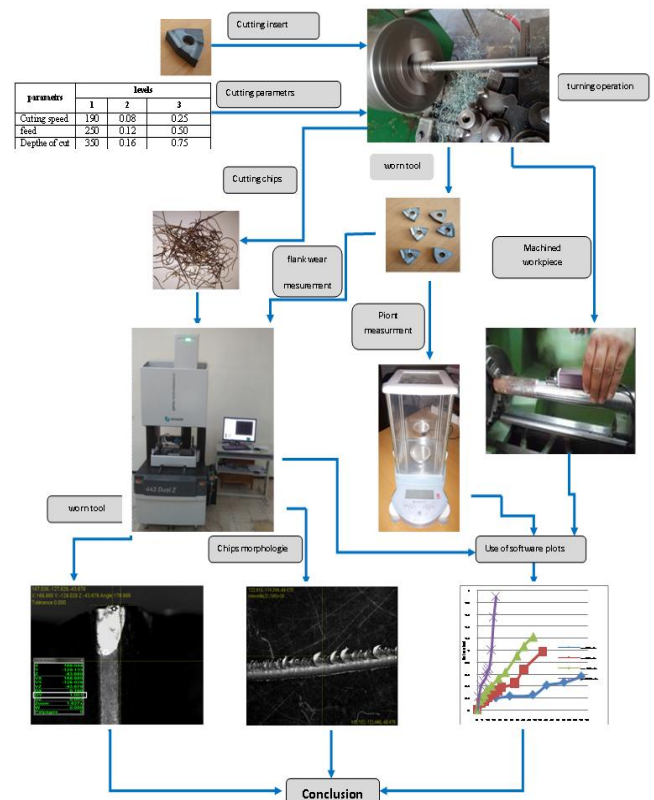


Fig. 4. Experimental setup

The study of the variation of flank wear, surface roughness and chip morphology as a function of the cutting speed leads to finding the values of these parameters mentioned in Table 3.

Table 3. Experimental conditions and results

Cutting speed (m/min)	Feed rate (mm / rev)	Depth of cut (mm)	N° of pass	Flank wear (mm)	Surfaces roughness ( $\mu\text{m}$ )
380	0.08	0.5	1	0.1	1.72
			2	0.12	1.71
			3	0.15	1.75
			4	0.18	1.81
			5	0.2	2.18
			6	0.23	2.30
			7	0.25	2.17
			8	0.41	2.18
			9	0.46	2.57
			10	0.56	2.58
620	0.08	0.5	1	0.11	1.61
			2	0.15	1.77
			3	0.21	1.90
			4	0.26	1.95
			5	0.29	2.09
			6	0.32	2.05
			7	0.38	2.20
			8	0.45	2.60
			9	0.68	2.69
			10	0.98	2.76
760	0.08	0.5	1	0.15	0.91
			2	0.2	0.94
			3	0.25	1.21
			4	0.34	1.71
			5	0.4	1.93
			6	0.53	2.10
			7	0.63	2.15
			8	0.91	2.57
			9	1.07	3.61
			10	1.23	4.48
1100	0.08	0.5	1	0.22	0.84
			2	0.41	0.93
			3	0.48	1.34
			4	0.54	2.21
			5	0.62	3.18
			6	0.67	3.49
			7	0.7	4.26
			8	1	5.33
			9	1.56	5.46
			10	1.9	5.53

### 3. RESULTS AND DISCUSSIONS

#### 3.1 Direct measurement of flank wear

The evaluation of flank wear is assessed by direct measurement. The measure is carried out using the three-dimensional measuring machine 443 Dual Z (Figure 2). The measurement is made after each pass.

For testing the tool life the standard ISO 3685 (1993) is respected.

The evaluation of flank wear is effected by its direct measurement. This is taken from the first use of the cutting inserts to the end of their service life.

Figures 5 (a), (b) and (c) represent the visualizations carried out after a time of use of the turning inserts of: 6 min, 48 min and 90 min respectively, and with the following cutting conditions:  $V_c=380$  m/min,  $f=0.08$  mm/rev and  $a_p=0.5$  mm.

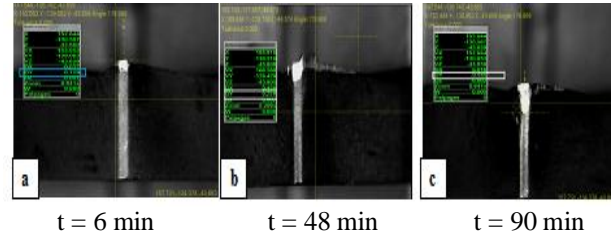


Fig.5. Visualization of VB tool face wear after cutting ( $V_c = 380$  m/min,  $f = 0.08$  mm / rev and  $a_p = 0.5$  mm)

Figures 6 (a), (b) and (c) represent the visualizations carried out after a time of use of the turning inserts of: 18 min, 32 min and 56 min respectively, and with the following cutting conditions:  $V_c=620$  m/min,  $f=0.08$  mm/rev and  $a_p=0.5$  mm.

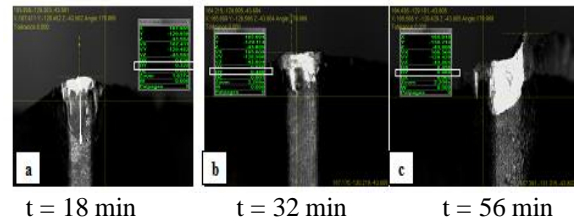


Fig. 6. Visualization of VB tool face wear after cutting ( $V_c = 620$  m/min,  $f = 0.08$  mm/rev and  $a_p = 0.5$  mm)

Figures 7 (a), (b) and (c) represent the visualizations carried out after a time of use of the turning inserts of: 4 min, 34 min and 48 min respectively, and with the following cutting conditions:  $V_c=760$  m/min,  $f=0.08$  mm/rev and  $a_p=0.5$  mm.

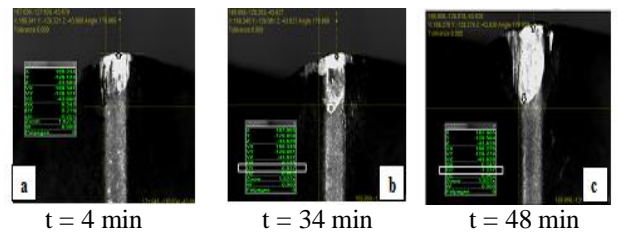


Fig. 7. Details of VB wear on the tool face after machining ( $V_c = 760$  m/min,  $f = 0.08$  mm / rev and  $a_p = 0.5$  mm)

Figures 8 (a), (b) and (c) represent the visualizations carried out after a time of use of the turning inserts of: 3 min, 10 min and 16 min respectively, and with the following cutting conditions:  $V_c=1100$  m/min,  $f=0.08$  mm/rev and  $a_p=0.5$  mm.

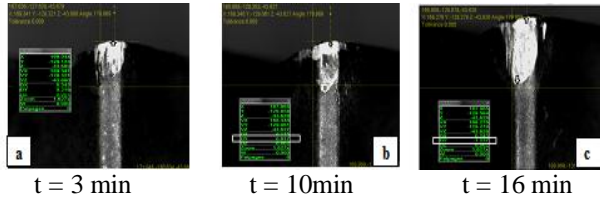


Fig.8. Details of VB wear on the tool face after machining ( $v_c = 1100$  m/min,  $f = 0.08$  mm/rev and  $a_p = 0.5$  mm)

The analysis of Figure 5, Figure 6, Figure 7 and Figure 8 shows that the universal law of wear of any mechanical part is observed (running-in, normal wear, accelerated wear). The figures also show clearly that the cutting speed has an important impact on the wear of the cutting tools, and with this, the increase in cutting speed results in a remarkably higher wear. At the end of chaque experiment (after 10 pass) the cutting edge is completely collapsed. Wear is very rapid and very severe. However, in the dry turning tests, tool wear is regular over time and at different cutting speeds. Figure 9 represents the evolution of the flank wear of the cutting inserts as a function of the cutting time at various levels of the cutting speed, always keeping the feed and the depth of cut constant.

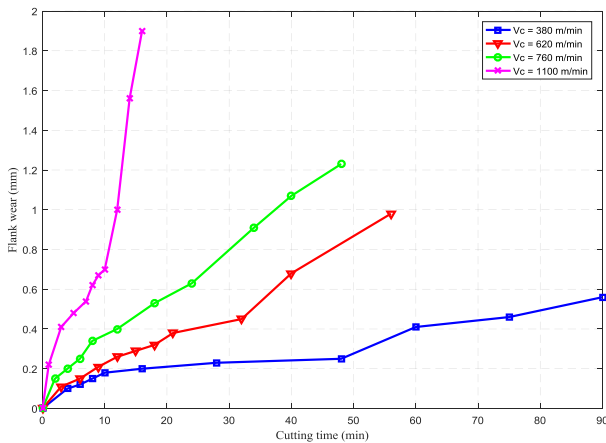


Fig. 9. Flank wear (VB) function of cutting time  $f = 0.08$  mm/rev, and  $a_p = 0.5$  mm

In the present study, the tool life (maximum permissible machining time) is planned from the flank wear. For each machining trials, fresh cutting tools are used, the progression of wear curve is recorded for every cutting time (T) and experiments are conducted until tool life criteria (VB) reaches 0.40 mm. Average measured flank wear (VB) based on machining time is shown in Figure 8. The flank wear value increases rapidly with cutting time at high cutting speeds. On the contrary, the progression of the tool flank wear curve is slow for low cutting speed speeds. Two different stages are observed in the wear curves.

The normal wear rate increases steadily over time, as shown by experiments at cutting speeds 380, 620 and 760 m/min.

Therefore, for the cutting speed  $V_c = 380$  m/min,

normal wear extends over a period of 60 min, while for the cutting speeds 620 m/min and 760 m/min it extends to 30 min and 18 min respectively; at a high cutting speed  $V_c = 1100$  m/min, the normal wear zone is almost non-existent the increase in speed causes accelerated wear. This is probably due to the rise in temperature in the work piece.

### 3.2 Influence of wear on durability and productivity

Figure 10 shows the representation of flank wear (VB) as a function of time for the different cutting speeds used to define tool life. It is noted that the tool life (T) has been determined based on flank wear. These tool life values are measured on the bases of two admissible wear values  $VB = 0.4$  mm and  $VB = 0.6$  mm.

The evaluation of the performance of the tool life shows that for cutting speeds varied between 380 and 620 m/min, when the speed ratio is of the order of 1.63, the tool life is reduced by 41%. It is also observed that with a speed varying from 620 to 760 m/min, with a variation ratio of 1.22, the tool life decreases by 56%. Finally and for a cutting speed varying in a higher range 760 to 1100 m / min, the tool life of the corresponding tool is reduced by 80%.

From the above, it is concluded that the tool life is highly dependent on the variation in cutting speed.

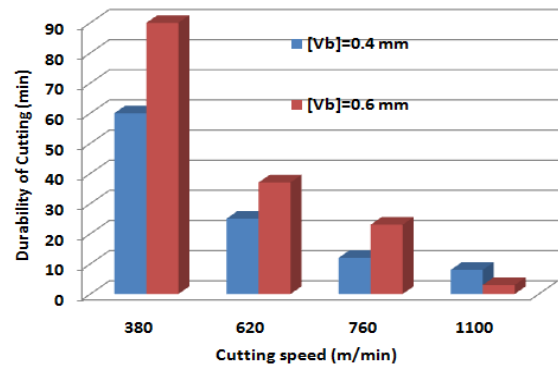


Fig.10. Durability (T) for two wear criteria  $VB = 0.4$  mm and 0.6 mm ( $f = 0.08$  mm/rev,  $a_p = 0.5$  mm)

Figure 10 shows a reduction in cutting tool life with increasing cutting speed. This reduction in tool life at high cutting speeds is due to the high temperatures generated by the cutting process at the tooltip, which favors the various wear mechanisms (abrasion and diffusion), and consequently, the tool's cutting capacity is reduced.

This can also be explained by the fact that when cutting at high speeds, the stresses on the cutting edge increase due to mechanical and thermal loads. Wear is caused by contact and high pressure at the interface between the tool and the chip and the tool and the workpiece.

### 3.3 Indirect measurement of flank wear

Indirect measurement of wear is intended for volumetric measurement due to the weight reduction of the cutting insert.

The variation in the mass of the cutting turning inserts after machining operations, as a function of the cutting time, is illustrated in Figures 11 (a), (b), (c) and (d).

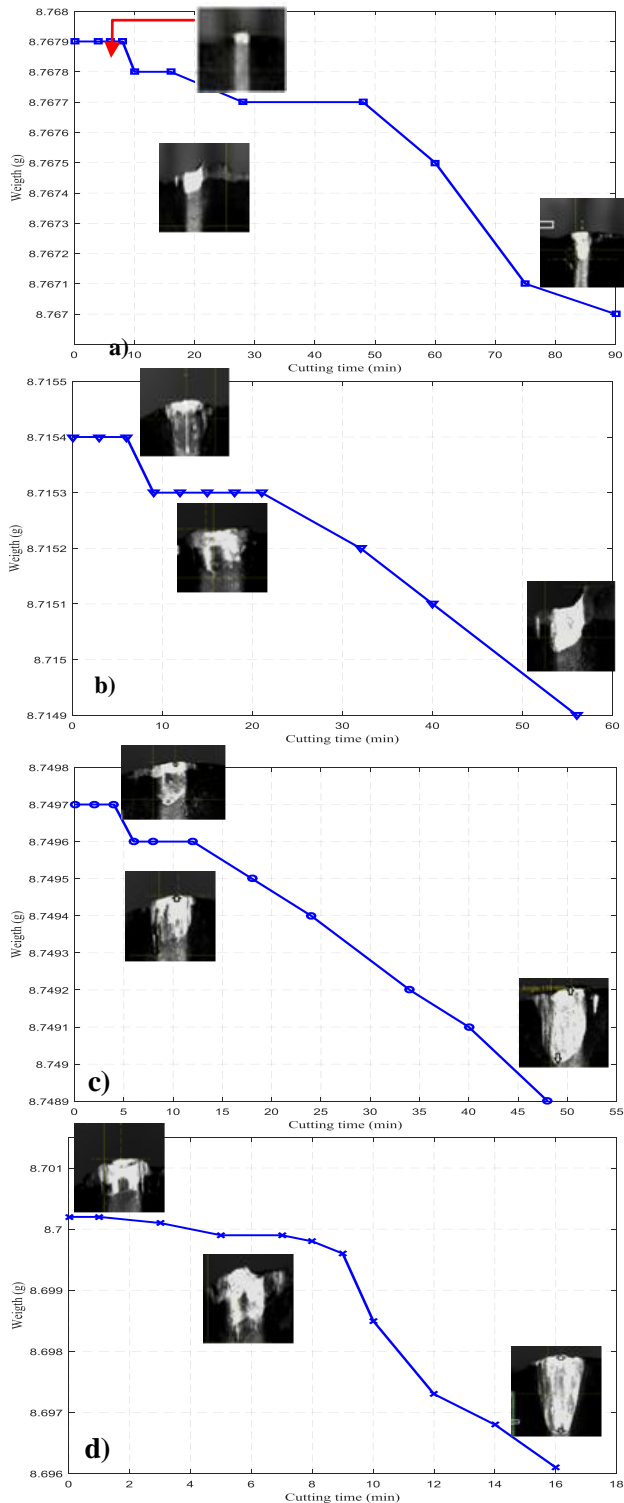


Fig. 11. Measuring wear due to reduction in tool weight in relation to cutting time ( $f=0.08\text{mm/rev}$ ,  $a_p=0.5\text{mm}$ )

The analysis of the assembly of Figure 10, allowed concluding that the wear of the cutting tool passes through three stages. The first stage characterized by a curve of low slope, this curve presents the mass lost during the cutting and consequently the wear of the insert is low. In the second stage, the weight loss is

almost negligible which results in zero or stable wear. This stage is long for low cutting speeds. However, at the final stage, it is observed that the slope of the weight loss curve is high, which means that the wear is rapid.

For better understanding, the weight variation values obtained, for a cutting time vary from 0 to 50 min at a cutting speed of 380 m/min; are almost unchanged, and as the machining time increases, the tool weight decreases almost linearly (VB between 0.2 and 0.4). Beyond a cutting time value equal to 50 min, the weight of the insert decreases considerably, which is the appearance of rapid wear.

The speed of 620 m/min causes practically no change in mass before a cutting time of 20 minutes, beyond this value of the cutting time there is a remarkable change in mass, which can be explained, from Figure 9, by a variation linear wear from 0.26mm to 0.38 mm. As in the two preceding cases, the use of the speed 760 m/min involves practically any change in weight, before a cutting time of 10 minutes. After 10 min of cutting, a change in weight occurs, which is explained, as indicated in Figure 9, by the linear variation of wear from 0.15 mm to 0.4 mm. With a cutting speed of 1100 m/min, the change in weight occurs if the machining time exceeds 9 min and it continues to increase during machining. This is explained by a linear wear curve tending to increase from 0.22 mm to 0.62 mm according to Figure 9.

Figure 11 shows the loss of weight produced during the machining of AISI T1 steel at different cutting speeds for the two wear criteria  $VB=0.4\text{ mm}$  and  $0.6\text{ mm}$ .

In cutting experiments, an increase in cutting speed leads to a reduction in tool life. Examination of Figure 12 shows that at a speed of 380 m/min a long cutting time is required to wear out the cutting insert. Therefore, almost the same trend was observed for a cutting speed of 620 m/min. However, a short cutting time is sufficient to wear out the cutting edge for cutting speeds of the order of 760 m/min and 1100 m/min during. Therefore; the conclusion drawn is more that the cutting speed is high the reduction in tool life is significant.

These results show that cutting speeds of 380; 620 m/min leads to a longer tool life.

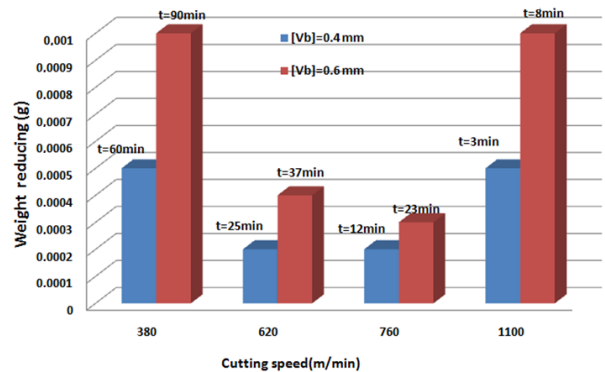


Fig. 12. Weight reducing for two wear criteria  $[VB]=0.4\text{ mm}$  and  $0.6\text{ mm}$  ( $f=0.08\text{ mm/rev}$ ,  $a_p=0.5\text{ mm}$ )

### 3.4 Microscopic analysis of chips

For each cutting speed, microscopic observations of chips produced during machining were made. The aim of this experimental analysis is to be able to compare the mechanisms of chip formation during cutting operations.

Figures 13, 14, 15 and 16 represent the observation of the morphology of the chips; this observation is carried out on an optical microscope of the CMM type, equipped with a CCD camera.

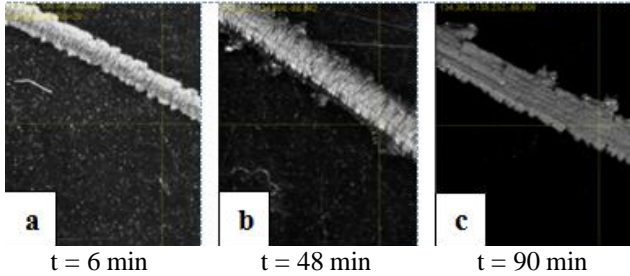


Fig. 13. Chip morphology ( $V_c = 380$  m/min,  $f = 0.08$  mm/rev, and  $a_p = 0.5$  mm)

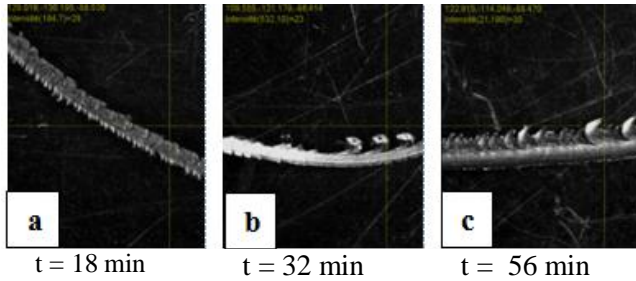


Fig. 14. Chip morphology ( $V_c = 620$  m/min,  $f = 0.08$  mm/rev, and  $a_p = 0.5$  mm)

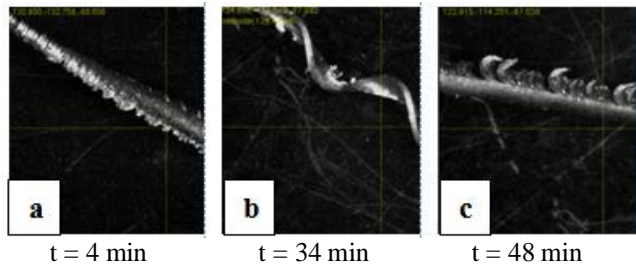


Fig. 15. Chip morphology ( $V_c = 760$  m/min,  $f = 0.08$  mm/rev, and  $a_p = 0.5$  mm)

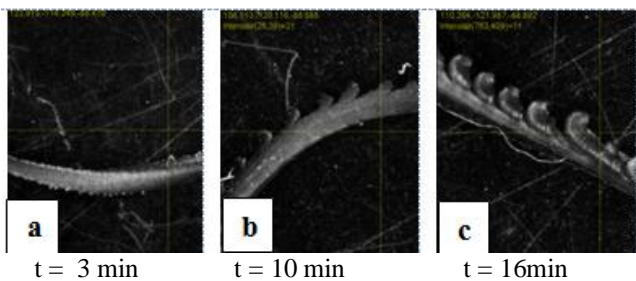


Fig. 16. Chip morphology ( $V_c = 1100$  m/min,  $f = 0.08$  mm/rev, and  $a_p = 0.5$  mm)

The study of the morphology of the chips at the microscopic scale is carried out following conventional cutting tests. This chip morphology varies essentially as a function of the speed and the

cutting time. Three forms of chips were observed: continuous, discontinuous (segmented) or detached (elementary chips).

Figures 13, 14, 15 and 16 provide the microscopic visualization of the chips produced when turning AISI T1 steel using a tungsten carbide cutting tool. The images record different types of chips generated according to different cutting speeds after different machining times.

The chips formed showed minimal plastic deformation. It was found that with continuous contact between the tool and workpiece and during the increase in machining time, the chips formed were more tense and continuous. The chip morphology confirms the formation of saw-tooth type chips with severe serration due to the cyclic propagation of cracks caused by plastic deformation. Continuous chips resulted in higher abrasive forces on the cutting tool. However, the chips formed during the process produced reaction forces on the face of the tool which reduced the tool life. Staining in chip color is also observed due to a high surface temperature.

Chip analysis shows that cutting speed and cutting time have a significant influence on chip morphology. Certainly, turning AISI T1 steel at low speed makes it possible to obtain continuous chips, this continuity is due to plastic deformation in the shear zones. It should be noted that with the increase in the cutting speed ( $V = 1100$  m/min), the chip thickness is more and more scalloped. This means that it takes with time, the form of the saw teeth due to cyclic cracking by creating shear bands very intense. There is also variation in the color of the chips due to the high surface temperature.

### 3.5 Effects of wear on roughness

The curves of Figures 17 (a), (b), (c) and (d) illustrate the variation in the surface roughness as a function of the cutting time, for cutting speeds of 380 m/min; 620 m/min; 760 m/min and 1100 m/min successively.

After each pass, and with the four cutting speeds, the roughness of the machined surfaces is measured using a roughness meter.

The analysis of the curves representing the surface roughness as a function of the cutting time leads to the conclusion that at cutting speeds of 380, 620 m/min the roughness of the surface remains almost stable at first time, then it is slowly increases after a cutting time (60 min using a cutting speed of 380 m/min and 20 min using a cutting speed of 620 m/min).

On other hand, for cutting speeds of 760 m/min and 1100 m/min, the surface roughness increases significantly during the cutting operation. Roughness values with these cutting speeds are important after the last two passes.

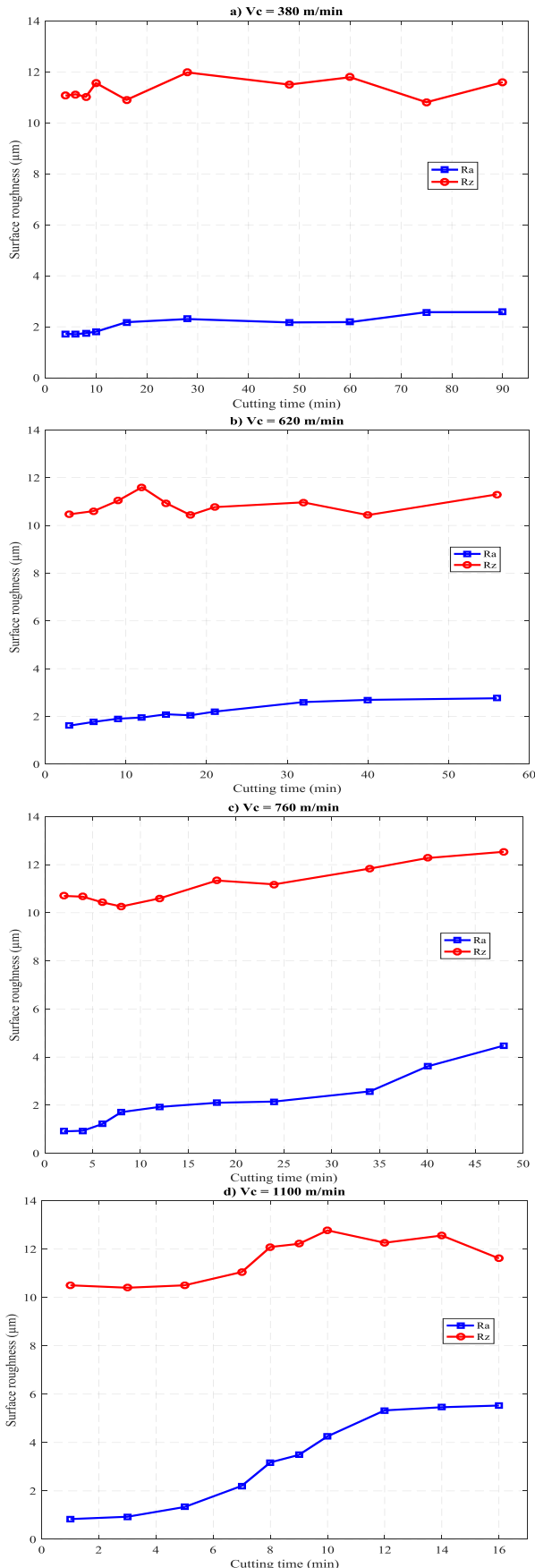


Fig. 17. Roughness as a function of time ( $f=0.08\text{mm/rev}$ ,  $a_p=0.5\text{mm}$ ) (a)  $V_c=380\text{m/min}$ ; (b)  $V_c=620\text{m/min}$ ; (c)  $V_c=760\text{m/min}$ ; (d)  $V_c=1100\text{m/min}$

By linking Figures 17 (a), (b), (c) and (d) with Figure 9, it is concluded that the increase in the flank wear VB produces a degradation of the quality of the machined surface.

It should be noted here that, while the flank wear is regular and does not exceed the value  $VB = 0.4\text{ mm}$ , the surface roughness (in particular the criteria Ra and Rz) changes very slowly and the surface quality remains appreciable.

Indeed, the Ra values recorded does not exceed the value of  $3\text{ }\mu\text{m}$  for the different cutting speeds tested. Beyond this value of VB the surface roughness undergoes a relative increase. Therefore, increased flank wear VB leads to a damage of the facets surface and cutting edges of the tool, which leads to a deterioration of the machined surface quality.

Analysis of the results shows that the roughness value (Ra, Rz) is not stable and not uniform during cutting. This instability is closely related to the flank wear. It can therefore be said that the damage to the facets surface of and cutting edges leads to a degradation of the machined surface.

The analysis of the curves also shows that the insert used ensures a good finish of the machined surface after a long machining time.

With a cutting speed of  $760\text{ m/min}$  and after a cutting time of 4 min the roughness value ( $R_a$ ) did not exceed the value of  $1\text{ }\mu\text{m}$ , likewise, with a higher cutting speed  $V_c = 1100\text{ m/min}$  and after a time of 3 min the roughness value ( $R_a$ ) did not exceed the value of  $1\text{ }\mu\text{m}$ .

In fact, a higher cutting speed leads to an acceleration of wear and consequently an increase in the value of the roughness, this result in the abrasion effect due to the contact between the tools and the part and the increase in the cutting temperature at the tool-chip workpiece interface.

#### 4. CONCLUSIONS

This research work investigated the influence of cutting speed on the life of tungsten carbide turning inserts when dry turning AISI T1 steel. The microscopic analysis of VB wear shows that the most distinguished wear phenomenon is abrasive wear, which is characterized by the appearance of grooves on the flank of the tool, due to the friction of the machined surfaces with the surfaces of the active part of the tool. Therefore, the speed range of  $[380-760]\text{ m/min}$  can be considered as an optimal operating range (long tool life) of tungsten carbide tools when machining AISI T1 steel. The high cutting speed of around  $1100\text{ m/min}$  is not recommended due to the rapid wear of the tool, resulting in too short a tool life.

The performance of the cutting turning inserts during dry turning of AISI T1 steel was examined, the wear clearance of the tool face VB for each cutting speed



is modified by varying the cutting time, indeed; The monitoring of the values of the roughness of the machined surfaces and the analysis of the chips morphology showed that an increase in the level of chips segmentation due to a local change in the insert geometry. This change related to the tool wear. The monitoring of wear, the surface roughness and the chips morphology made it possible to identify the wear mechanisms and the tool life.

## 5. REFERENCES

- Alagan, N.T., Zeman, P., Hoier, P., Beno, T., Klement, U., (2019). *Investigation of micro-textured cutting tools used for face turning of alloy 718 with high-pressure cooling*, Journal of Manufacturing Processes, **37**, 606-616.  
<https://doi.org/10.1016/j.jmapro.2018.12.023>
- Traxel, K. D., Bandyopadhyay, A. , (2019). *First Demonstration of Additive Manufacturing of Cutting Tools using Directed Energy Deposition System: Stellite™-Based Cutting Tools*, Additive Manufacturing, **25**, 460-468.  
<https://doi.org/10.1016/j.addma.2018.11.019>
- Venkatesan, K., (2017). *The study on force, surface integrity, tool life and chip on laser assisted machining of inconel 718 using Nd:YAG laser source*, Journal of Advanced Research, **8**, 407-423.  
<https://doi.org/10.1016/j.jare.2017.05.004>
- Hoier, P., (2017). *Characterization of WC-Co tools used for machining of Alloy 718 under the influence of high-pressure coolant supply*, Phd thesis, Department of Industrial and Materials Science, Chalmers University of Technology, Gothenburg.
- Diniz, A.E., aMachado Á. R. , Corrêa, J. G. , (2016). *Tool wears mechanisms in the machining of steels and stainless steels*, International Journal of Advanced Manufacturing Technology, **87**, 3157–3168.<https://doi.org/10.1007/s00170-016-8704-3>.
- Hood, R., Soo, S. L. , Aspinwall, D. K. , Mantle, A. L. , (2018). *Tool life and workpiece surface integrity when turning an RR1000 nickel based superalloy*, The International Journal of Advanced Manufacturing Technology, **98**, 2461–2468.  
<https://doi.org/10.1007/s00170-018-2371-5>
- Schultheiss, F., Bushlya, V., Lenrick, F., Johansson, D., Kristiansson, S., Ståhl, J. E. , (2018). *Tool Wear Mechanisms of pcBN tooling during High-Speed Machining of gray cast iron*, Procedia CIRP, **77**, 606-609.  
<https://doi.org/10.1016/j.procir.2018.08.201>
- Ayed, Y., (2013). *Approches expérimentales et numériques de l'usinage assisté jet d'eau haute pression: étude des mécanismes d'usure et contribution à la modélisation multi-physiques de la coupe*, Phd thesis, Ecole nationale supérieure d'arts et métiers, ENSAM.
- Abdelkrim, M., Brioua, M., Belloufi, A., Brabie, G., (2016). *Numerical study of cutting temperature during drilling process of the c45 steel*, International Journal of Modern Manufacturing Technologies, **VIII**(2), 42-47.
- Fnides, B., Boutabba, S., Fnides, M., Aouici, H., Yallese, M., (2013). *Cutting tools flank wear and productivity investigation in straight turning of X38CrMoV5 (50HRC)*, International Journal of Applied Engineering and Technology, **3**(1), 2277-212, <http://www.cibtech.org/jet.htm>.
- Serra, R., Rmili, W., (2016). *Experimental Evaluation of Flank Wear in Dry Turning from Accelerometer Data*, International Journal of Acoustics and Vibrations, **21**(1), 50-58.  
10.20855/ijav.2016.21.139.
- Alagan, N. T., Hoier, P., Zeman, P.I, Klement, U., Beno, T., Wretland, A., (2019). *Effects of high-pressure cooling in the flank and rake faces of WC tool on the tool wear mechanism and process conditions in turning of Alloy 718*, Wear, **434-435**, 102922, <https://doi.org/10.1016/j.wear.2019.05.037>
- Odedeyi, P.B., Abou-El-Hossein, K., Liman, M., (2017). *An experimental study of flank wear in the end milling of AISI 316 stainless steel with coated carbide inserts*, Journal of Physics: Conference Series, **843**, 012058, <https://doi.org/10.1088%2F1742-6596%2F843%2F1%2F012058> .
- Mallesha, V., Hanumanthappa, S., Badiger, P., Mahesh, V., (2019). *Machinability Studies On En47 Spring Steel by Optimization Technique During Dry And Wet Condition*; International Journal of Modern Manufacturing Technologies, **XI**(2), 9, 2067-3604.
- Jahanbakhsh, M., Akhavan Farid, Mohammad Lotfi, A., (2016). *Optimal flank wear in turning of Inconel 625 super-alloys using ceramic tool*; Proceedings of the Institution of Mechanical Engineers, Part B: Journal of Engineering Manufacture, **232**.  
<https://doi.org/10.1177/0954405416640698>
- Ibrahim, G.A., Che Haron, C. H. , Ghani, J. A. , Moh. Said, A. Y. , Moh. Z. Abu Yazid, (2011). *Performance of PVD-Coated Carbide Tools When Turning Inconel 718 in Dry Machining*, Advances in Mechanical Engineering, **2011**.  
<https://doi.org/10.1155/2011/790975>
- D'Addona, D.M., Matarazzo, D., SharifUllah, A.M.M., Teti, R., (2015). *Tool wear control through cognitive paradigms*, Procedia CIRP, **33**, pp. 221-226.  
<https://doi.org/10.1016/j.procir.2015.06.040>
- J. M. Paiva et al., (2017). *Tribological and Wear Performance of Carbide Tool with TiB2 PVD Coating under Varying Machining Conditions of TiAl6V4 Aerospace Alloy*, Coatings, **7**(11), pp. 187, <https://doi.org/10.3390/coatings7110187>

19. Narasimha, M., Ramesh, S., (2014). *Coating Performance on Carbide Inserts*, International Journal of Engineering and Technical Research, **2**(8), 175-179.
20. Chin, T., Song, L., Li, S., Liu, X. (2019). *Experimental Study on Wear Characteristics of PCBN Tool with Variable Chamfered Edge*, Chinese Journal of Mechanical Engineering, **32**(37). <https://doi.org/10.1186/s10033-019-0351-9>
21. Sharma, V., Pandey, P.M., (2016). *Recent advances in ultrasonic assisted turning: A step towards sustainability*, Cogent Engineering, **3**(1), pp. 1222776. <https://doi.org/10.1080/23311916.2016.1222776>
22. Tiwari, K., Shaik, A., Arunachalam, N., (2018). *Tool wear prediction in end milling of Ti-6Al-4V through Kalman filter based fusion of texture features and cutting forces*, Procedia Manufacturing, **26**, pp. 1459-1470. <https://doi.org/10.1016/j.promfg.2018.07.095>
23. Hua, Y., Liu, Z., (2018). *Effects of cutting parameters and tool nose radius on surface roughness and work hardening during dry turning Inconel 718*, International Journal of Advanced Manufacturing Technology, **96**, 2421–2430, <https://doi.org/10.1007/s00170-018-1721-7>.
24. Anthymidis, K.G., (2011). *Wear of cutting tools used in milling treatments*, Key Engineering Materials, **465**.
25. Yaltese, M. A., (2007). *Investigation expérimental sur l'usure des outils de coupe en CBN lors du tournage des pièces dures*, Sciences & Technologie, B – N°26.
26. Das, S. R., Panda, A., Dhupal, D., (2017). *Experimental investigation of surface roughness, flank wear, chip morphology and cost estimation during machining of hardened AISI 4340 steel with coated carbide insert*, Mechanics of Advanced Materials and Modern Processes, **3**(9). <https://doi.org/10.1186/s40759-017-0025-1>
27. Rosemar, B. S., Machado, Á. R., Ezugwu, E. O., Bonney, J., Sales, W. F., (2013). *Tool life and wear mechanisms in high speed machining of Ti-6Al-4V alloy with PCD tools under various coolant pressures*, Journal of Materials Processing Technology, **213**(8), 1459-1464, <https://doi.org/10.1016/j.jmatprotec.2013.03.008>.
28. Toller-Nordström, L., (2019). *Insights into wear and deformation of alternative binder hardmetals*, Digital Comprehensive Summaries of Uppsala Dissertations from the Faculty of Science and Technology, 1373, pp. 77, ISBN 978-91-513-0789-3.
29. Ben Abdelali, H., (2013). *Caracterisation et modelisation des mecanismes tribologiques aux interfaces outils-pieces-copeaux en usinage a sec de l'acier c45*, Phd thesis, Ecole Centrale de Lyon.
30. Wang, W., Hong, G. S., Wong, Y., Zhu, K., (2007). *Sensor fusion for online tool condition monitoring in milling*, International Journal of Production Research, **45**, 5095-5116. [10.1080/00207540500536913](https://doi.org/10.1080/00207540500536913).
31. Srithara, A., Palanikumar, K., Durgaprasad, B., (2014). *Experimental Investigation and Surface roughness Analysis on Hard turning of AISI D2 Steel using Coated Carbide Insert*, GCMM, Procedia Engineering, **97**, pp. 72-77. <https://doi.org/10.1016/j.proeng.2014.12.226>
32. Ahmad, A.F., Nuawi, M.Z., Abdullah, S., Wahid, Z., Karim, Z., Dirhamsyah, M., (2015). *Development of tool wear machining monitoring using novel statistical analysis method, I-kazTM*, Procedia Engineering, **101**, pp. 355 – 362. <https://doi.org/10.1016/j.proeng.2015.02.043>
33. Cakan, A., Fatih, E., Vedat, O. (2015). *Data-driven simulations of flank wear of coated cutting tools in hard Turning*, Mechanics, **21**. <https://doi.org/10.5755/j01.mech.21.6.12199>

---

Received: April 30, 2020 / Accepted: December 15, 2020 / Paper available online: December 20, 2020 © International Journal of Modern Manufacturing Technologies